Potential Field Function based Vehicle Lateral Stability Control

MIAN ASHFAQ ALI[1], ABDUL MANAN KHAN[2], CHANG-SOO HAN[3*]
Department of Mechatronics Engineering Hanyang University[1]
Department of Mechanical Design Engineering Hanyang University[2]
Department of Robot Engineering Hanyang University[3]
Address: Sa-3 dong, Ansan South Korea
ishfaqaries@gmail.com, kam@hanyang.ac.kr cshan@hanyang.ac.kr[*], http://crnlab.re.kr

Abstract: - It is well known fact that narrower vehicles have more susceptibility to rollover and lateral stability. For the purpose of experimenting and analysis when certain additional weight is added to the vehicle then the C.G changes which can result in vehicle rollover. In this study a novel braking based methodology is used to devise a strategy on g-g diagram to modify the driver's commands of longitudinal acceleration in accordance with lateral acceleration to lateral stability. Potential field function is used to couple the lateral and longitudinal dynamics of vehicle for the purpose of lateral stability. The same method is applicable to mobile platform in autonomous mode of operation with ensured rollover stability.

Key-Words: - Potential Field Function, Electric Vehicle, Lateral Stability, Rollover Prevention.

1 Introduction

Vehicle rollover is a dangerous safety related issue for passenger vehicles as well as heavy trucks. NHTSA data shows a large number of fatalities are due to single vehicle accidents resulting from rollover when a vehicle takes sharp turn at high speed. This motion results into large lateral acceleration at the center of gravity. Previously researchers have established several metrics for the detection of vehicle rollover [1-4] and rollover prevention/mitigation schemes [1-2,5-8] once the rollover danger is detected. Vehicle rollover control can be achieved using differential braking control [9-11] which will results in decrease in both the yaw rate and vehicle velocity. In another study front and rear wheel steering system [12] is used for rollover stability. Active suspension and active antiroll-bar control [13-14] are also proposed.

It is well known that narrower vehicle are more prone to rollover than wider ones. Also for laboratory experimental work any additional weight changes the location of CG and safety margin for rollover or lateral stability also changes. One such example is the addition of batteries for studying of motion control of electric vehicle with narrow wheel base. In such situation the vehicle/mobile platform can rollover at much slow speeds at sharp turns. In this article novel method is proposed to couple the lateral dynamics of vehicle with its longitudinal dynamics on the phase portrait of g-g diagram. Potential field function is used to couple the lateral and longitudinal dynamics. G-vectoring control [15-18] was proposed to extract the behavior of an expert driver on a g-g diagram. In this study it is utilized to prevent rollover couple the dynamics.

2 Problem Formulation

Vehicle rollover can be prevented by differential braking, steering system, active suspension/antiroll-bar, and braking. These techniques reduces the yaw rate, roll angle and/ velocity of vehicle. If the vehicle yaw rate is corrected by the controller during obstacle avoidance maneuver then the vehicle cannot fulfill the driver intended trajectory and will follow some other path. This can cause accident. Second approach is to slow down the vehicle to a speed where centrifugal forces are small to prevent rollover. For example sharp turns can be executed at slower speeds. Rollover can be prevented by keeping the lateral acceleration of vehicle under constraints thought out its motion. On the other hand the vehicle going very slow and no danger of rollover does not seem to the right choice. So the solution is moving at higher speeds and keeping the lateral acceleration under constraints. The vehicle lateral acceleration a_y and longitudinal acceleration a_x are coupled together on g-g diagram using potential field function for this purpose.

2.1 Relationship between Rollover and Lateral Acceleration

For the detection of rollover rollover index (RI) is used as defined in Eq.1. Rollover index represent the difference between vertical tire forces at left and right wheels. As the vertical tire forces cannot be directly measured so rollover index can be estimated

using Eq. 2. This equation is based on roll dynamics model of vehicle. The same equation can be further simplified by neglecting the second term who effect is small as compared with first term in Eq.2. Eq.4 shows the lateral acceleration at which the wheel lift occurs. It is clear from this equation that rollover is dependent of vehicle geometric parameters along with lateral acceleration. By keeping the lateral acceleration at lower values the danger of rollover can be suppressed.

$$RI = \frac{F_{zr} - F_{zl}}{F_{zr} + F_{zl}} \quad -1 < RI < 1 \tag{1}$$

$$RI = \frac{2h}{t.g} a_y \cos\phi + \frac{2h}{t} \sin\phi \tag{2}$$

$$RI \cong \frac{2h}{t.g} a_y \tag{3}$$

$$a_{y\_lift\_off} = \left(\frac{t}{2h} \right).\mathrm{g} \tag{4}$$

2.2 Lateral Acceleration Constraints

The vehicle lateral acceleration can be calculated using Eq. 5 and by neglecting the second term of sliding Eq.6 can be utilized.

$$a_y = V_x \cdot \gamma + \ddot{y} \tag{5}$$

$$a_y \cong V_x \cdot \gamma \tag{6}$$

The lateral acceleration given in Eq.6 is maintained by controlling the speed and imposing the constraints as given in Eq.4. Given a value of lateral acceleration and using Eq.6 the plot on vehicle velocity and yaw rate can be plotted as shown in Fig.1. If the vehicle motion stays below this plot then the value of lateral acceleration will not exceed and lateral stability can be ensured.

3 Vehicle Modeling and Verification

The electric vehicle details model is developed in TruckSim. It is rear drive vehicle with in-wheel motors fitted in each rear wheel that can be control independently.

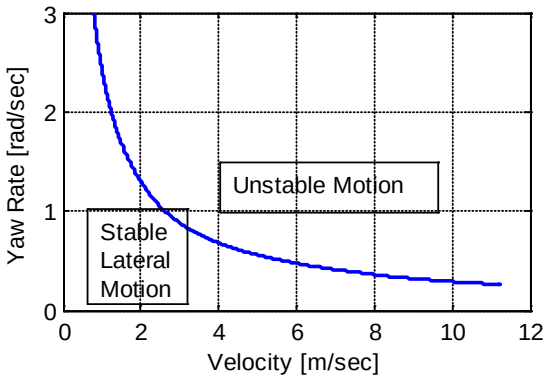

Figure 1. Vehicle Velocity vs Yaw Rate

3.1 Vehicle Dynamic Model

In this study full vehicle model is used in simulation. EV COMS (Toyota Company) electric vehicle model parameters were used to develop this model. The actual vehicle and its model is shown in Figure 2.

(a) (b)

Figure 2. EV COMS Electric Vehicle with In-wheel Motor and EVCOMS Vehicle Dynamics Model

This full-vehicle model consists of sprung mass dynamic model, front wheel steering system model, four independent suspension models and four wheel dynamics models. Here, sprung mass dynamic model has three translational and three rotational degrees of freedom (DOFs). Wheel dynamics model contain the motor model, braking system model and tire model. The DOF information of different components of the vehicle model is listed in Table 1.

Table 1. Degree of Freedom of Full-vehicle Model

	Number of parts	Degree of freedom
Body(Sprung Mass)	1	6
Steering Model	1	1
Suspension Model	4	4
Wheel Dynamic Model	4	4
Total		15

Table 2 shows the physical parameters of vehicle model i.e. vehicle mass, wheel tread, wheelbase, tire radius, and yaw moment of inertia used in simulations. The full vehicle model has a total of three inputs, two torque commands for each rear wheel and steering wheel angle command for front wheels.

Table 2. Parameters for Electric Vehicle with In-wheel Motor used in Simulation

Parameter	Unit	Specification
Vehicle Mass	kg	345
Wheel Base	mm	1725
Tread	mm	Front : 840 Rear : 815
Distance from C.G to Front Axle	mm	838
Distance from C.G to Rear Axle	mm	895
Tire Radius	mm	220
Yaw Moment of Inertia	kgm^2	160
In-wheel Electric Motor (2EA)	KW	1

3.2. Motor Dynamic Model

The in-wheel motor drive electric vehicle with the four-wheel driving system has four in-wheel motors, one in each wheel. As each wheel can be control independently, so differential driving and braking can be realized. In this study, in-wheel-motor is modeled using the first order transfer function as given in Eq.7.

$$T_m(s) = \frac{K_t/R_m}{1+(L_m/R_m)s} U_m(s) = \frac{1}{1+(L_m/R_m)s} T_{m\_com}(s) \quad (7)$$

The output torque T_m of motor model is determined by the input value that is the wheel torque command T_{m_com} from the control algorithm. Figure 3 (a) shows the motor performance curve that was the result of motor testing. The data of Figure 3 (b) was used for simulation purpose.

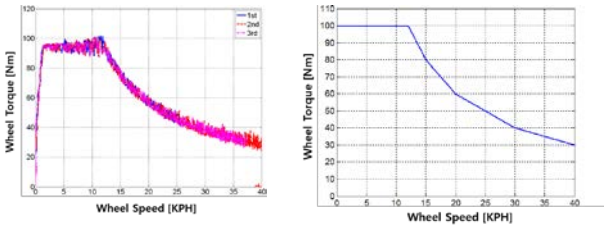

(a) Motor Test Data (b) Look up Table Data

Figure. 3. Motor Performance Curve

3.3. Vehicle Model Verification

The verification of vehicle model was done in a simple double lane change test at 15kph. We have compared the simulation and experimental data of vehicle yaw rate and lateral acceleration for double lane change test. At first, the experiment of double lane change was performed on dry asphalt road on test vehicle and data of steering angle sensor along with yaw rate, lateral acceleration and vehicle velocity were recorded on the notebook and then the same data of steering wheel angle input was used in double lane change simulation at the same vehicle speed and data of vehicle yaw rate and lateral acceleration was recorded again.

The simulation and experimental conditions are shown in Table 3 and the vehicle yaw rate and lateral acceleration data comparison is shown in Figure 4 for verification purpose. This data comparison shows very close agreement between the vehicle model and test vehicle.

Table 3 Simulation & Experimental Conditions for Vehicle Model Verification

Condition	Value
Vehicle Model Verification	Double Lane Change Test at 15kph
Vehicle Speed in Experiments	25 kph (Fixed Speed)
Road Condition	Split-mu Road Left (μ=0.85) Right (μ=0.40)
Experiment/Test	Straight Motion on split-mu

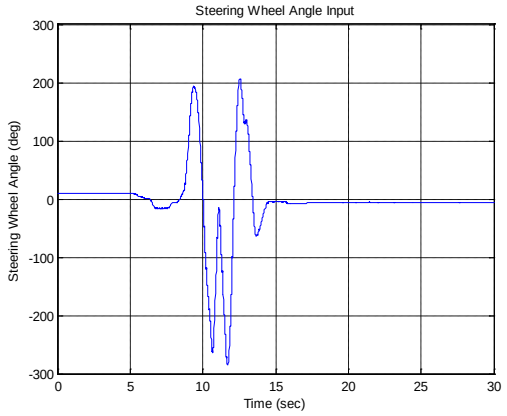

(a) Steering Wheel Angle Input

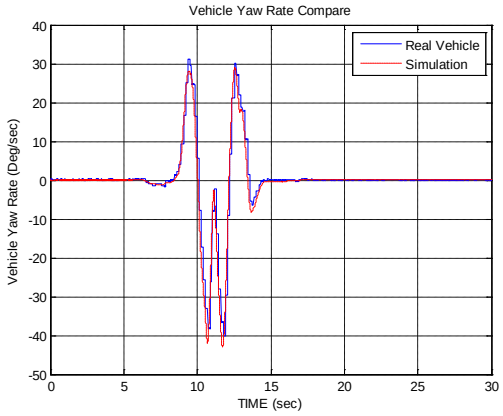

(b) Vehicle Yaw Rate

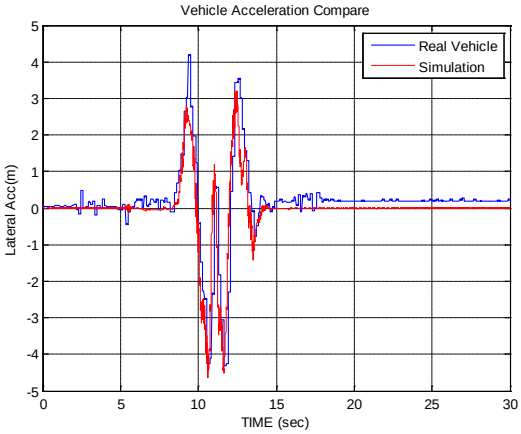

(c) Vehicle Lateral Acceleration

Figure. 4. Double Lane Change Test Comparison between a Test Vehicle and a Full Vehicle Model.

4 Problem Solution

The strategy proposed in this article is the lateral acceleration is always under the constraint of limiting value of lateral acceleration as given by Eq.4. The driving control algorithm is shown in Figure 5. The potential field function calculates the save longitudinal acceleration on the basis of difference between the actual lateral acceleration and limiting value of later acceleration.

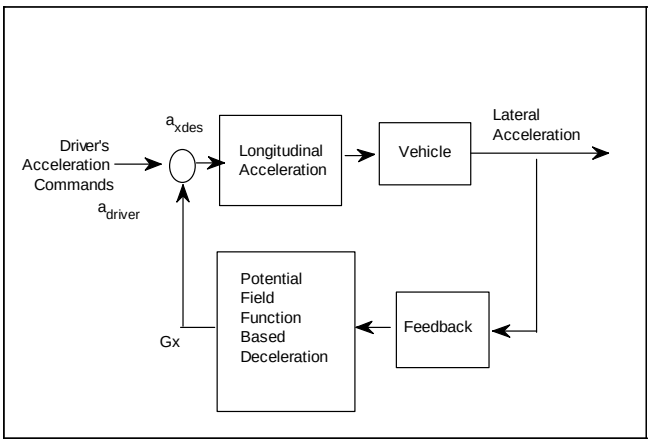

Figure. 5. Driving Control Algorithm for Lateral Stability

Originally this method is used in mobile robotics for obstacle avoidance where the distance from the obstacle is measured and if its within predefined radius range then a virtual repulsive force is generated that modify the mobile planned path. Using the same concept the vehicle is decelerated on the basis of difference between the actual lateral acceleration and limiting lateral acceleration at which the rollover is likely to happen. The limiting lateral acceleration is treated like an obstacle and the system will use torque control to avoid this value of lateral acceleration by slowing down the vehicle. This deceleration will be generated if the difference between the actual lateral acceleration and limiting acceleration is less than a predefined gap as shown in Eq. 9. Within this range this algorithm will generate more deceleration as the actual lateral acceleration goes more close to the limiting value of lateral acceleration and the driver's command of desired acceleration will be modified.

The *signum* function takes into account the signs of lateral acceleration and roll angle. Their combine effect can be additive or can cancel the effect of each other if they are of opposite signs.

$$G_x = -\mathrm{sgn}\left(a_y, \phi\right).\frac{1}{2}.\eta\left(\frac{1}{\left(a_y - a_{y\_\lim}\right)} - \frac{1}{\Delta_{a_y}}\right) \tag{8}$$

$$a_{des} = \begin{cases} a_{driver} - G_x & , \ \left(a_y - a_{y\_\lim}\right) < \Delta_{a_y} \\ a_{driver} & , \ \left(a_y - a_{y\_\lim}\right) > \Delta_{a_y} \end{cases} \tag{9}$$

5 Simulation

The performance of the driving control algorithm is evaluated in simulation. The algorithm is developed in Simulink and vehicle model which is developed in TruckSim is run in close loop with Simulink. The following simulations are conducted with and without utilizing the controller action of modifying the driver's acceleration commands..

5.1 Steering Step Input at 40 kph

The vehicle is started from zero initial velocity and after attaining the desired velocity the step steering input of 240 degrees is applied. This will produce lateral acceleration value of 0.53 g. In this simulation the limiting value 0.35 g of lateral acceleration constraints is enforced using this concept. The two cases compared in the following plots. Velocity comparison is shown in Fig.6.

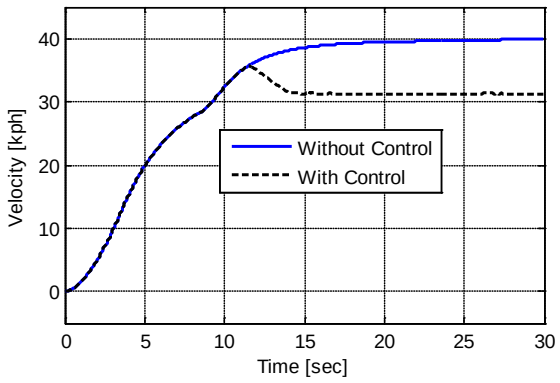

Figure. 6. Velocity Comparison for Steering Step Input at 40 kph

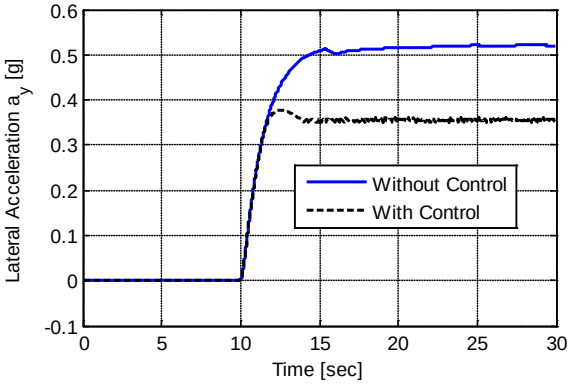

Figure. 7. Lateral Acceleration Comparison for Steering Step Input at 40 kph

The potential field function will decelerate the vehicle using Eq. 8 and velocity will be reduced and as a result lateral acceleration will be reduced as well. The lateral acceleration is plotted in Fig.7 and the corresponding performance on g-g diagrams is shown in Fig. 8. In Fig.9 the controller action cause the vehicle to stay in the stable motion region while the vehicle without control passes the lateral acceleration limit as shown in Fig. 9.

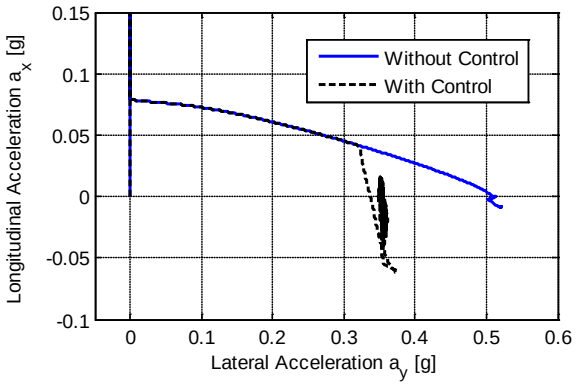

Figure. 8. g-g diagram for Steering Step Input at 40 kph

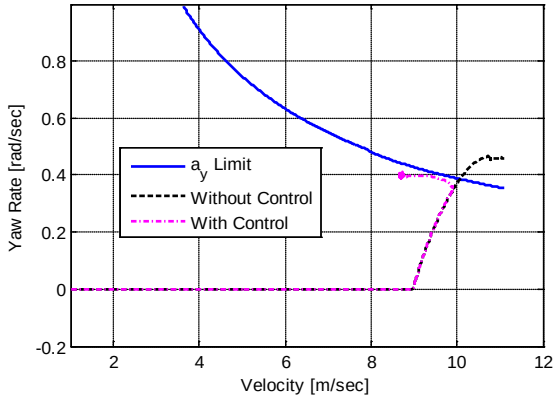

Figure. 9. Control Performance on Velocity-Yaw Rate Plot for Steering Step Input at 40 kph

5.2 Steering Ramp Input at 40 kph

The vehicle is started from zero initial velocity and after attaining the desired velocity the ramp steering input is applied as shown in Fig. 10.

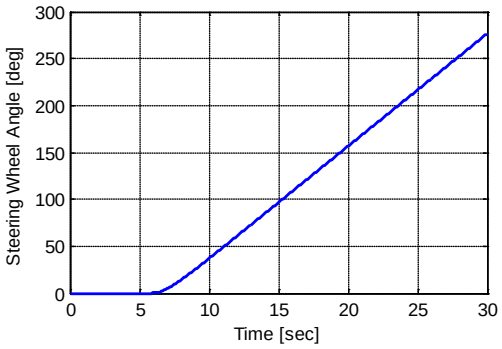

Figure. 10. Steering Ramp Input at 40 kph

The ramp steering input will increase the yaw rate and lateral acceleration as shown in Fig. 12. The purpose of this simulation is to evaluate the controller performance to slowly increasing lateral acceleration. For this simulation the two cases of with and without controller action are compared and plots for velocity, lateral acceleration, trajectory and g-g diagrams are shown.

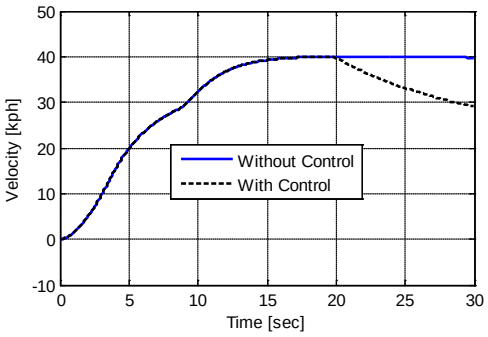

Figure. 11. Velocity Comparison for Steering Step Input at 40 kph

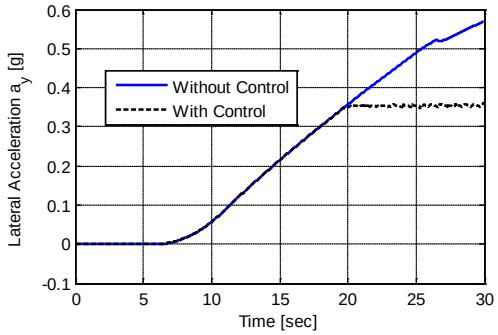

Figure. 12. Lateral Acceleration Comparison for Steering Ramp Input at 40 kph

It is clear from the Fig.14 that the controller impose the 0.35g lateral acceleration value and causes deceleration in order to prevent the lateral acceleration to cross the limiting value. The trajectory is shown in Fig. 13 in which the controlled vehicle travels less distance due to low velocity. Fig. 15 shows the performance on Velocity-Yaw Rate plot. The controller action cause the vehicle lateral acceleration to stay below the limiting value while in case of no controller the vehicle follows the driver commands of acceleration and yaw rate and enter into the region of unstable motion.

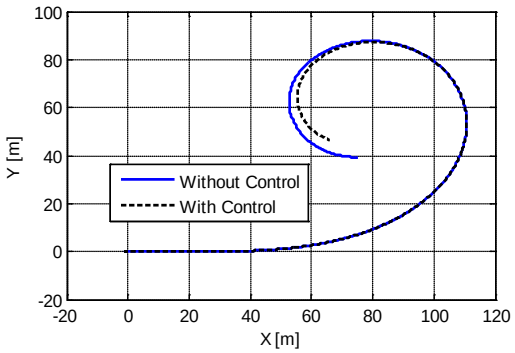

Figure. 13. Vehicle Trajectory Comparison for Steering Ramp Input at 40 kph

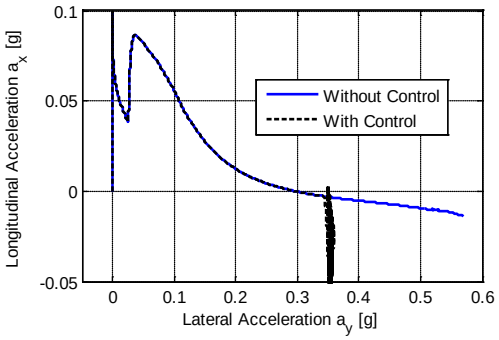

Figure. 14. g-g diagram for Steering Ramp Input at 40 kph

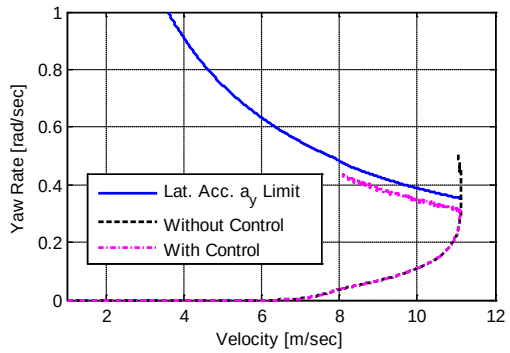

Figure. 15. Control Performance on Velocity-Yaw Rate Plot for Steering Ramp Input at 40 kph

6 Conclusion

In this study a novel strategy is devised for lateral stability of a class of vehicle which are more susceptible to rollover at lower values of lateral acceleration. The potential field function is used to couple the longitudinal and lateral vehicle dynamics in a way that the lateral acceleration will be under some desired constraints. The two simulations of step steering input and ramp input shows that this methodology can ensure the maintaining lateral acceleration under desired constraints. This method can also be applied to mobile robots for autonomous mode of operation.

References:

[1] H. Yu, L. Güvenc, and Ü. Özgüner, "Heavy duty vehicle rollover detection and active roll control," *Vehicle system dynamics*, vol. 46, no. 6, pp. 451-470, 2008.

[2] J. Yoon, D. Kim, and K. Yi, "Design of a rollover index-based vehicle stability control scheme," *Vehicle System Dynamics*, vol. 45, no. 5, pp. 459-475, 2007.

[3] E. Dahlberg, A method determining the dynamic rollover threshold of commercial vehicles, *SAE Technical Paper*, 2000.

[4] B.-C. Chen, and H. Peng, "Rollover warning for articulated heavy vehicles based on a time-to-rollover metric," *Journal of dynamic systems, measurement, and control*, vol. 127, no. 3, pp. 406-414, 2005.

[5] J. Yoon, S. Yim, W. Cho, B. Koo, and K. Yi, "Design of an unified chassis controller for rollover prevention, manoeuvrability and lateral stability," *Vehicle System Dynamics*, vol. 48, no. 11, pp. 1247-1268, 2010.

[6] J. Yoon, W. Cho, B. Koo, and K. Yi, "Unified Chassis Control for Rollover Prevention and Lateral Stability," *IEEE Transactions on Vehicular Technology*, vol. 58, no. 2, pp. 596-609, 2009.

[7] C. Larish, D. Piyabongkarn, V. Tsourapas, and R. Rajamani, "A New Predictive Lateral Load Transfer Ratio for Rollover Prevention Systems," *IEEE Transactions on Vehicular Technology*, vol. 62, no. 7, pp. 2928-2936, 2013.

[8] J. Cao, L. Jing, K. Guo, and F. Yu, "Study on Integrated Control of Vehicle Yaw and Rollover Stability Using Nonlinear Prediction Model," *Mathematical Problems in Engineering*, vol. 2013, pp. 15, 2013.

[9] B. C. Chen, and H. Peng, "Differential-braking-based rollover prevention for sport utility vehicles with human-in-the-loop evaluations," *Vehicle System Dynamics*, vol. 36, no. 4-5, pp. 359-389, Nov, 2001.

[10] V. Cherian, R. Shenoy, A. Stothert, J. Shriver, J. Ghidella, and T. D. Gillespie, Model-Based Design of a SUV anti-rollover control system, *SAE Technical Paper*, 2008.

[11] B. Lee, A. Khajepour, and K. Behdinan, Vehicle stability through integrated active steering and differential braking, *SAE Technical Paper*, 2006.

[12] T. Shim, and D. Toomey, Investigation of active steering/wheel torque control at the rollover limit maneuver, *SAE Technical Paper*, 2004.

[13] P. Ponticel, "Dynamic testing rollover on the way," *Automotive Engineering International*, pp. 26-28, 2003.

[14] A. Hac, Influence of active chassis systems on vehicle propensity to maneuver-induced rollovers, *SAE Technical Paper*, 2002.

[15] M. Yamakado, J. Takahashi, S. Saito, A. Yokoyama, and M. Abe, "Improvement in vehicle agility and stability by G-Vectoring control," *Vehicle System Dynamics*, vol. 48, pp. 231-254, 2010.

[16] M. Yamakado, K. Nagatsuka, and J. Takahashi, "A yaw-moment control method based on a vehicle's lateral jerk information," *Vehicle System Dynamics*, vol. 52, no. 10, pp. 1233-1253, 2014.

[17] J. Takahashi, M. Yamakado, S. Saito, and A. Yokoyama, "A hybrid stability-control system: combining direct-yaw-moment control and G-Vectoring Control," *Vehicle System Dynamics*, vol. 50, no. 6, pp. 847-859, 2012.

[18] J. Takahashi, M. Yamakado, and S. Saito, "Evaluation of preview G-vectoring control to decelerate a vehicle prior to entry into a curve," *International Journal of Automotive Technology*, vol. 14, no. 6, pp. 921-926, Dec, 2013.

Nomenclature

T_m	Output Torque of Motor
T_{m_com}	Wheel Torque Command
L_m	Motor Coil Inductance
R_m	Motor Coil Resistance
s	Laplase Operator
δ	Steering Wheel Angle
ϕ	Roll Angle
a_x, a_y	Longitudinal and Lateral Acceleration
$a_{y\_lift\_off}$	Lateral Acceleration at which Wheel Lift Off the ground
$a_{y\_\lim}$	Limiting Value of Lateral Acceleration
a_{driver}	Driver's Commanded Longitudinal acceleration
a_{des}	Resultant Longitudinal Acceleration
G_x	Acceleration by Potential Field Function
RI	Rollover Index
t	Tread
h	Sprung Mass C.G Height
g	Gravity
η	Tuning Gain